

Supporting Information

Increase of 3rd-Order Nonlinear Optical Activity of PbS Quantum Dots in Zeolite Y by Increasing Cation Size

Hyun Sung Kim and Kyung Byung Yoon *

Korea Center for Artificial Photosynthesis, Center for Microcrystal Assembly,
Department of Chemistry, Sogang University,
Seoul 121-742, Korea

Contents

- SI-1. Representative 3-NLO Materials
- SI-2. The Reason Why [(PbS)_{QD}, 2H⁺]_Y is Acidic
- SI-3. Experimental Procedure
- SI-4. Calculation Bases
- SI-5. Measurement of 3-NLO Activity
- SI-6. Z-scan Data at 532 nm
- SI-7. Z-scan Data at 1064 nm
- SI-8. Sanderson's Partial Negative Charge of Oxygen in the Zeolite Framework
- SI-9. Methods Used to Prepare Figure 4

SI-1. Representative 3-NLO Materials

Metal Cluster Nanocomposites

Material	λ (nm)/ τ_i/τ_r	γ^a	β^a	Ref.
Cu/SiO ₂	532/6ps/100Hz	3.0		1
Cu/SiO ₂	527/6ps/1Hz	4.8	850	2
Cu/SiO ₂	527/55ps/2Hz		6000	2
Cu/Al ₂ O ₃	596/6ps/3.8M	293.0	-2.34×10^4	3,4
Cu/Al ₂ O ₃	1064/55ps/2Hz	-17.0		5
Cu/ZnO	532/55ps/2Hz		3.54×10^5	6
Au/SiO ₂	500/30ps/10Hz	5.0		7
Au/SiO ₂	559/30ps/10Hz		-2.4×10^4	7
Au colloids	532/35ps/10Hz	4.8	~ 0.01	8
Au/Al ₂ O ₃	1064/55ps/2Hz	-146.0		5
Ag/ SiO ₂	532/55ps/2Hz	-620.0	-6.7×10^4	9

^a $\times 10^{-12}$ cm²/W, ^bcm/GW.

Organic and Organometallic Materials

Material	λ (nm)/ τ_i/τ_r	γ^a	β^a	Ref.
Azobenze-PVA	532/38ps/10Hz	-82.9		10
Azobenze-PVA	1064/38ps/10Hz	4.85		10
BuCu/PMMA	532/20ps/10Hz	-4.15	-300	11
BuCu/PMMA	1064/20ps/10Hz	-1.71	107	11
LC	532/38ps/10Hz	-110		12
polyaniline	532/70ps/10Hz	-4	0.002	13
azopolymer	532/38ps/10Hz	-9.46	-285.3	14
azopolymer	1064/38ps/10Hz	-4.57		14
Zn Pc	532/6ns/10Hz		47.74	15
La Pc	532/6ns/10Hz		95.46	15
Nd(Pc) ₂	532/6ns/10Hz		42	15
Ga(Pc) ₂	532/6ns/10Hz		33.5	15

^a $\times 10^{-12}$ cm²/W, ^bcm/GW.

Carbon Materials

Material	λ (nm)/ τ_i/τ_r	γ^a	β^a	Ref.
CNT	532/45ps/10Hz	-	0.76	16
DWNT-C ₆₀	532/6ns/10Hz	-	7.01	17
C60 film	532/55ps/0.5H	900		18
C60 film	532/55ps/2Hz	-420	1.7×10^5	19
C60	1064/35ps/10H		0.22	20
C70	1064/35ps/10H		0.05	20

^a $\times 10^{-12}$ cm²/W, ^bcm/GW.

Semiconductor QDs

Material	λ (nm)/ τ_i/τ_r	γ^a	β^a	Ref.
PbSe	1064/50ps/1Hz		-4.7	21
PbS in silica-titania	1064/60ps/10Hz	-4.0		22
CdS	532/25ps/10Hz		0.2	23
Lead oxyhalide glass	532/80ps/10Hz		20	24
CdTe in glass	1064/50p/1Hz	-0.95	26	25
InP	1064/100ps/10Hz	-2.1	9	26
CdSe and CdSe/ZnS	1064/55ps	-0.5		27
GaAs in vycor glass	1064/55ps/1kHz	-5.6	26	28
GaAs in glass	1064/100ps/10Hz	-1.3	80	29
PbS	780/150fs/76MHz	-4.7		30
PbS-polymer	780/150fs/76MHz	6.8		31
PbS in PVA	532/50ps/1Hz	-6.2	-50	32
PbS in PVA	1064/50ps/1Hz	-1.0	45.7	32
NaNbO ₃ in glass	532/100ps/10Hz	-0.02		33
NaNbO ₃ in glass	1064/100ps/10Hz	0.01		33
ZnS	532/28ps/10Hz		0.2	34
As ₂ S ₃	1064/15ps/10Hz	0.05		35
As ₂ Se ₃	1064/15ps/10Hz	0.12		35

^a $\times 10^{-12}$ cm²/W, ^bcm/GW.

References

- (1) Battaglin, G.; Calvelli, P.; Cattaruzza, E.; Gonella, F.; Polloni, R.; Mattei, G.; Mazzoldi, P. *Appl. Phys. Lett.* **2001**, *78*, 3953.
- (2) Polloni, R.; Scremin, B. F.; Calvelli, P.; Cattaruzza, E.; Battaglin, G.; Mattei, G. *J. Non-Cryst. Sol.* **2003**, *322*, 300.
- (3) Ballesteros, J. M.; Serna, R.; Solis, J.; Afonso, C. N.; Petford-Long, A. K.; Osborne, D. H.; Haglund Jr, R. F. *Appl. Phys. Lett.* **1997**, *71*, 2445.
- (4) Ballesteros, J. M.; Solis, J.; Serna, R.; Afonso, C. N. *Appl. Phys. Lett.* **1999**, *74*, 2791.
- (5) Ganeev, R. A.; Ryasnyanskiy, A. I.; Stepanov, A. L.; Marques, C.; da Silva, R. C.; Alves, E. *Opt. Commun.* **2005**, *253*, 205.
- (6) Ryasnyanskiy, A.; Palpant, B.; Debrus, S.; Ganeev, R.; Stepanov, A.; Can, N.; Buchal, C.; Uysal, S. *Appl. Optics* **2005**, *44*, 2839.
- (7) Jun, H. S.; Lee, K. S.; Yoon, S. H.; Lee, T. S.; Kim, I. H.; Jeoung, J. H.; Cheong, B.; Kim, D. S.; Cho, K. M.; Kim, W. M. *Phys. Stat. sol.* **2006**, *203*, 1211.
- (8) Ganeev, R. A.; Ryasnyanskiy, A. I.; Kamalov, Sh. R.; Lodirov, M. K.; Usmanov, T. *J. Phys. D: Appl. Phys.* **2001**, *34*, 1602.
- (9) Ganeev, R. A.; Ryasnyanskiy, A. I.; Stepanov, A. L.; Usmanov, T. *Opt. and Quantum Elect.* **2004**, *36*, 949.
- (10) He, T.; Cheng, Y.; Du, Y.; Mo, Y. *Optics Comm.* **2007**, *275*, 240.
- (11) Fan, H.; Wang, X.; Ren, Q.; Li, T.; Zhao, X.; Sun, J.; Zhang, G.; Xu, D.; Sun, Z.; Yu, G. *Appl. Phys. A* **2010**, *99*, 279.
- (12) Zhang, X.; Wang, C.; Lu, X.; Zeng, Y. *J. Appl. Polym. Sci.* **2011**, *120*, 3065.
- (13) Maciel, G. S.; Bezerra Jr., A. G.; Rakov, N.; de Araújo, C. B.; Gomes, A. S. L. *J. Opt. Soc. Am. B* **2001**, *18*, 1099.
- (14) He, T.; Cheng, Y.; Wang, C.; Jia, T.; Li, P.; Mo, Y. *phys. stat. Sol. (b)* **2007**, *244*, 2166.
- (15) Venkatram, N.; Rao, D. N.; Giribabu, L.; Rao, S. V. *Appl. Phys. B* **2008**, *91*, 149.
- (16) Seo, J. T.; Ma, S. M.; Yang, Q.; Creekmore, L.; Battle, R.; Tabibi, M.; Brown, H.; Jackson, A.; Skyles, T.; Tabibi, B.; Jung, S. S.; Namkung, M. *J. Phys.: Conf. Series* **2006**, *38*, 37.
- (17) Jena, K. C.; Bisht, P. B.; Shaijumon, M. M.; Ramaprabhu, S. *Optics Comm.* **2007**, *273*, 153.
- (18) Ryasnyanskii, A. I. *Optics and Spectroscopy* **2005**, *99*, 126.
- (19) Ganeev, R. A.; Ryasnyanskiy, A. I.; Redkorechev, V. I.; Fostiropoulos, K.; Priebe, G.; Usmanov, T. *Optics Comm.* **2003**, *225*, 131.
- (20) Ganeev, R. A.; Ryasnyanskii, A. I.; Kodirov, M. K.; Kamalov, Sh. R.; Usmanov, T. *Optics and Spectroscopy* **2002**, *93*, 789.
- (21) Yu, B.; Zhu, C.; Xia, H.; Chen, H.; Gan, F. *J. mater. sci. lett.* **1997**, *16*, 2001.

- (22) Martucci, A.; Fick, J.; Schell, J.; Battaglin, G.; Guglielmi, M. *J. Appl. Phys.* **1999**, *86*, 79.
- (23) Han, M. Y.; Gan, L. M.; Huang, W.; Chew, C. H.; Zou, B. S.; Quek, C. H.; Xu, G. Q.; Ji, W.; Zhang, X. J.; Ng, S. C. *Talanta* **1998**, *45*, 735.
- (24) De Araujo, R. E.; de Araújo, C. B.; Poirier, G.; Poulain, M.; Messaddeq, Y. *Appl. Phys. Lett.* **2002**, *81*, 4694
- (25) Yu, B.; Zhu, C.; Gan, F. *J. Appl. Phys.* **2000**, *87*, 1759.
- (26) Dvorak, M. D.; Justus, B. L.; Gaskill, D. K.; Hendershot, D. G. *Appl. Phys. Lett.* **1995**, *66*, 804.
- (27) Gerdova, I.; Hache, A. *Optics Comm.* **2005**, *246*, 205.
- (28) Justus, B. L.; Tonucci, R. J.; Berry, A. D. *Appl. Phys. Lett.* **1992**, *61*, 3151.
- (29) Dvorak, M. D.; Justus, B. L.; Berry, A. D. *Optics Comm.* **1995**, *116*, 149.
- (30) Li, H. P.; Liu, B.; Kam, C. H.; Lam, Y. L.; Que, W. X.; Gan, L. M.; Chew, C. H.; Xu, G. Q. *Opt. Mater.* **2000**, *14*, 321.
- (31) Liu, B.; Li, H.; Chew, C. H.; Que, W.; Lam, Y. L.; Kam, C. H.; Gan, L. M.; Xu, G. Q. *Mater. Lett.* **2001**, *51*, 461.
- (32) Yu, B.; Yin, G.; Zhu, C.; Gan, F. *Opt. Mater.* **1998**, *11*, 17.
- (33) Falcão-Filho, E. L.; Bosco, C. A. C.; Maciel, G. S.; Acioli, L. H.; de Araújo, C. B.; Lipovskii, A. A.; Tagantsev, D. K. *Phys. Rev. B* **2004**, *69*, 134204.
- (34) Nikesh, V. V.; Dharmadhikari, A.; Ono, H.; Nozaki, S.; Kumar, G. R.; Mahamuni, S. *Appl. Phys. Lett.* **2004**, *84*, 4602.
- (35) Cherukulappurath, S.; Guignard, M.; Marchand, C.; Smektala, F.; Boudebs, G. *Opt. Comm.* **2004**, *242*, 313.

SI-2. The Reason Why $[(\text{PbS})_{\text{QD}}, 2\text{H}^+]_{\text{Y}}$ is Acidic

In the zeolite Y used in this study with the Si/Al ratio of 1.8, the number of H^+ is 67 per unit cell. Considering the volume of a unit cell ($1.51 \times 10^{-26} \text{ m}^3$), the pH of the zeolite in an aqueous solution corresponds to -0.87 .

SI-3. Experimental Procedure

Materials. Tetraethyl orthosilicate (TEOS, Acros), aluminum isopropoxide [Al(iPrO)₃, Aldrich], tetramethylammonium hydroxide (TMAOH, 25% aqueous solution, Aldrich), sodium silicate (Na₂SiO₃, 17-19% of Na₂O and 35-38% of SiO₂, Kanto), sodium aluminate (NaAlO₂, Na₂O = 31-35% and Al₂O₃ = 34-39%, Kanto), and sodium hydroxide (NaOH, Samchun) were used as received for preparation of zeolite Y film on the ITO glass (denoted as Y_f, Si/Al ratio = 1.8). Pb(NO₃)₂·4H₂O (Junsei), Li(NO₃)₂·6H₂O (Junsei), Na(NO₃)₂·6H₂O (Junsei), K(NO₃)₂·6H₂O (Junsei) and Rb(NO₃)₂·6H₂O (Junsei) were used as received. Dry H₂S and NH₃ gas were purchased from Regas.

Preparation of Y Films. The Y_fs (2 × 2.5 cm²) were prepared according to the procedure described in our previous report (xx) using ITO glass plates instead of ordinary glass plates. The average thickness of the pristine zeolite-Y films was 2.0 μm. After polishing them with a piece of fine cloth and 0.3-μm alumina powders, the pristine, opaque zeolite Y films became transparent and the average thickness decreased to 1.5 μm.

Preparation of [NH₄⁺/(PbS)₃₃]-Y_f. A Y_f was immersed into each 25-mL aliquot of Pb(NO₃)₂ solutions (10 mM) for 30 min at room temperature. The removed Pb²⁺-exchanged Y_f ([Pb]-Y_f) was washed with copious amounts of distilled deionized water, and dried by blowing nitrogen onto the film. The amount of Pb²⁺ ions per unit cell in each [Pb]-Y_f was 33, respectively. The [Pb]-Y_fs were then introduced into a Schlenk tube and then dried at 200 °C for 12 h under vacuum (< 10⁻⁵ Torr). Dry H₂S gas (Rigas, 99.5%) was introduced into the Schlenk tube containing dry [Pb]-Y_f plates at room temperature. After allowing them to react with dry H₂S for 1 h, excess H₂S gas was removed by evacuation of the Schlenk tube for 10 min at room temperature. Dry NH₃ gas (760 Torr) was subsequently introduced into the Schlenk tube at room temperature and it was allowed to react with the H⁺ in [H⁺/PbS]-Y for 20 min. This is designated as [NH₄⁺/PbS]-Y. The unreacted NH₃ gas in the tube was removed under vacuum at 60 °C for 6 h. The remaining trace amount of NH₃ gas was removed by purging with Ar and the subsequent evacuation for 1 h.

Preparation of [M⁺/(PbS)₃₃]-Y_f. First, 4 pieces of [NH₄⁺/(PbS)₃₃]-Y_fs were immersed into 30-mL of saturated NaNO₃ aqueous solutions for 1 day at room temperature for ion exchange

from NH_4^+ into Na^+ and was washed with copious amounts of DDW. 3 pieces of $[\text{Na}^+/\text{(PbS)}_{33}]\text{-Yfs}$ were immersed into the each MNO_3 aqueous solutions ($\text{M} = \text{Li, K, and Rb}$) for 1 day at room temperature for ion exchange from Na^+ into M^+ . After ion exchange process, each films was washed with copious amounts of distilled deionized water. The compositions were analyzed by energy dispersive X-ray spectroscopy (EDX) analyses.

Instrumentation. The θ - 2θ scans of Y films were performed on a Rigaku Ultima 4 with the power of 40 kV and 40 mA. The wavelength of the monochromated X-ray beam was 1.5406 nm generated from Cu $\text{K}\alpha$ radiation. Diffuse-reflectance UV-vis spectra of the samples were recorded on a Varian Cary 5000 UV-vis-NIR spectrophotometer equipped with an integrating sphere. The scanning electron microscope (SEM) images of zeolite films were obtained from a FE-SEM (Hitachi S4300) at an acceleration voltage 20 kV. A platinum/palladium alloy (in the ratio of 8 to 2) was deposited with a thickness of about 15 nm on top of the samples. The EDX analyses were obtained from a Horiba EX-220 Energy Dispersive X-ray Micro Analyzer (model: 6853-H) attached to the FE-SEM without coating the surface with a platinum/palladium alloy.

SI-4. Calculation Bases

1. Calculation of the number of PbS in 1.3 nm-PbS

(1) Density of PbS: 7.60 g/cm^3

(2) Molecular weight of PbS: 239.30 g/mole

(3) Weight of 1.3 nm sized PbS:

$$\text{Volume of 1.3 nm PbS: } 1,150 \text{ \AA}^3 \quad (1 \text{ \AA}^3 = 10^{-24} \text{ cm}^3)$$

$$(\text{Weight of 1.3 nm PbS}) / (1.15 \times 10^{-21} \text{ cm}^3) = 7.60 \text{ g/cm}^3$$

$$\text{Weight of total PbS} = 8.74 \times 10^{-21} \text{ g}$$

(5) Number of PbS molecules in 1.3 nm sized PbS:

$$(8.74 \times 10^{-21} \text{ g}) / (239.30 \text{ g/mole}) \times (6.02 \times 10^{23}) = 22$$

2. Calculation of the size of a PbS QD composed of 4 PbS units

(1) Density of PbS: 7.60 g/cm^3

(2) Molecular weight of PbS: 239.30 g/mole

(3) Weight of 4 PbS units: $(239.30 \text{ g/mole}) \times (4/6.02 \times 10^{23}) = 1.6 \times 10^{-21} \text{ g}$

(4) volume of 4 PbS units: $(1.6 \times 10^{-21} \text{ g} / V) = 7.60 \text{ g/cm}^3$

$$V = 2.11 \times 10^{-22} \text{ cm}^3 = 211 \text{ \AA}^3$$

$$4/3 \times 3.14 \times (r)^3 = 211 \text{ \AA}^3$$

$$r = 3.7 \text{ \AA} \quad (\text{diameter: } 7.4 \text{ \AA})$$

SI-5. Measurement of 3-NLO Activity

Measurements. The γ and β values of the samples were obtained by a z-scan technique at 532 and 1064 nm, respectively, using a mode-locked Nd:YAG laser of 50-ps pulse duration with the repetition rate of 10 Hz. The layout of z-scan method used in this work is as follows.

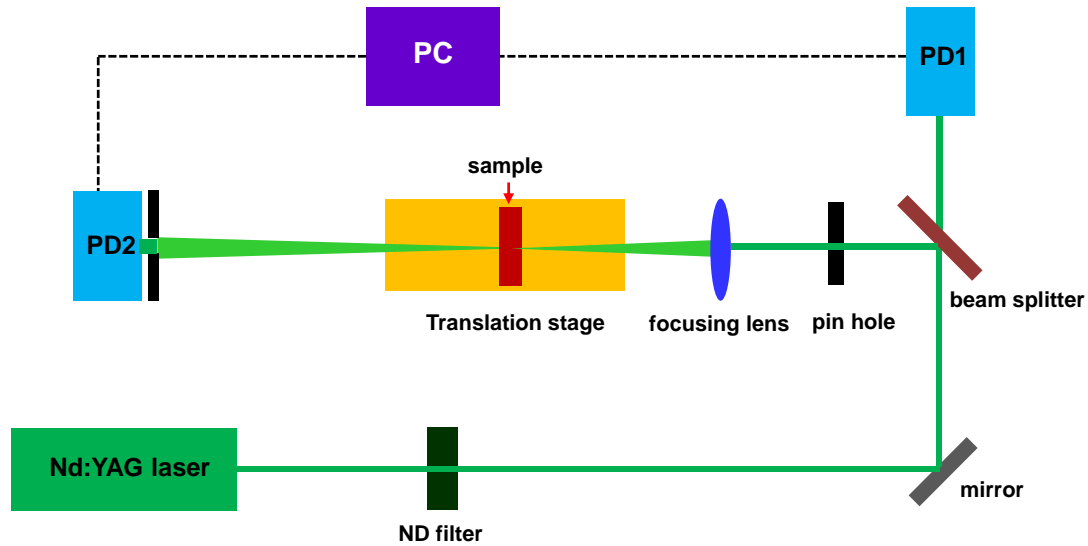


Fig. SI-5. The layout of z-scan method used in this work.

PD: Photodiode, ND filter: a neutral-density filter for the attenuation of beam power

The laser beam was split into two parts ($\sim 40\%$ and $\sim 60\%$) using a beam splitter. A part ($\sim 40\%$) of the beam was used to compensate the intensity fluctuation of individual laser pulses. The other part ($\sim 60\%$) was focused using a convex lens (focal length = 20 cm) and directed to the sample. The sample was placed on a stepping-motor-driven translational stage which can traverse along the on-axis of the focused beam in a unit interval of 1 mm. The intensity of the transmitted beam was measured using a Si photodiode (PIN-10D, UDT sensors). In the case of open-aperture z-scan, the whole energy of the transmitted beam was measured. In the case of on-axis (closed-aperture) z-scan measurement, an iris was placed in front of the detector. To satisfy the criteria for the on-axis transmittance, the diameter of the iris aperture was made to be 2 mm so that only 1 % of the transmitted beam was collected by the detector.

The on-axis z-scan measurement of CS_2 was first conducted to obtain the Rayleigh length (z_0) and the beam intensity at the focal point (I_0) of our laser beam for a give λ . For this,

CS₂ was contained in a quartz cell with the path length of 1 mm. Subsequently, the z-scan data of CS₂ were fitted with eq 1

$$T(z) = 1 + \frac{4q}{(1+q^2)(9+q^2)} \Delta\phi - \frac{2(3+q^2)}{(1+q^2)(9+q^2)} \Delta\psi \quad (1)$$

where, $q = z/z_0$, z = the longitudinal distance from the focal point, $\Delta\phi = (2\pi/\lambda)I_0\gamma L_{\text{eff}}$, and $\Delta\psi = \beta I_0 L_{\text{eff}}$, in which L_{eff} = the effective interaction length of the sample. Since the above fitting gives z_0 and $\Delta\phi$ values, the I_0 value was determined from $\Delta\phi = (2\pi/\lambda)I_0\gamma L_{\text{eff}}$ using the known γ value of CS₂ (3.0×10^{-14} cm²/W) and the known L_{eff} of CS₂ (1 mm) for a given λ . The obtained z_0 and I_0 values from the above measurements were 0.3 cm and 1.32 GW/cm² at 532 nm, respectively, and 0.31 cm and 2.14 GW/cm² at 1064 nm, respectively.

The L_{eff} values of [(PbS)_n]-Y/G and [(PbSe)_n]-Y/G for a given λ were obtained from eq 2 using the linear absorption coefficient and the film thickness (L) of each film, which were measured using a UV-vis spectrophotometer (Varian Carey 5000) and a field-emission scanning electron microscope, respectively.

$$L_{\text{eff}} = \frac{1 - e^{-\alpha L}}{\alpha} \quad (2)$$

The $\Delta\phi$ and $\Delta\psi$ values of [(PbS)_n]-Y/G and [(PbSe)_n]-Y/G were obtained by fitting their measured on-axis and open-aperture z-scan data with eq 1 and eq 3, respectively.

$$T(z) = 1 - \frac{1}{(1+q^2)} \Delta\psi \quad (3)$$

The corresponding γ and β values of the zeolite films were determined from the $\Delta\phi$, $\Delta\psi$, z_0 , I_0 , and L_{eff} values obtained above. Since the spatial profiles of our laser beams are very close to Gaussian (M^2 value < 1.2), the system errors in obtaining the significant numbers would be less than 10%.

The threshold powers that start damaging the samples were obtained by irradiating the samples for 5 min at varying beam powers for a given wavelength and examining the surfaces with a SEM. The SEM images of zeolite were obtained from a FE-SEM. On top of the samples platinum/palladium alloy (in the ratio of 8 to 2) was deposited with a thickness of about 15 nm. The energy dispersive X-ray spectroscopy (EDX) analyses were obtained from

a Horiba EX-400 EDX analyzer attached on the FE-SEM. The UV-vis-NIR spectra (both absorption and diffuse reflectance modes) were recorded from a Varian Cary 5000 UV-VIS-NIR spectrophotometer equipped with an integrating sphere.

SI-6. Z-scan Data at 532 nm

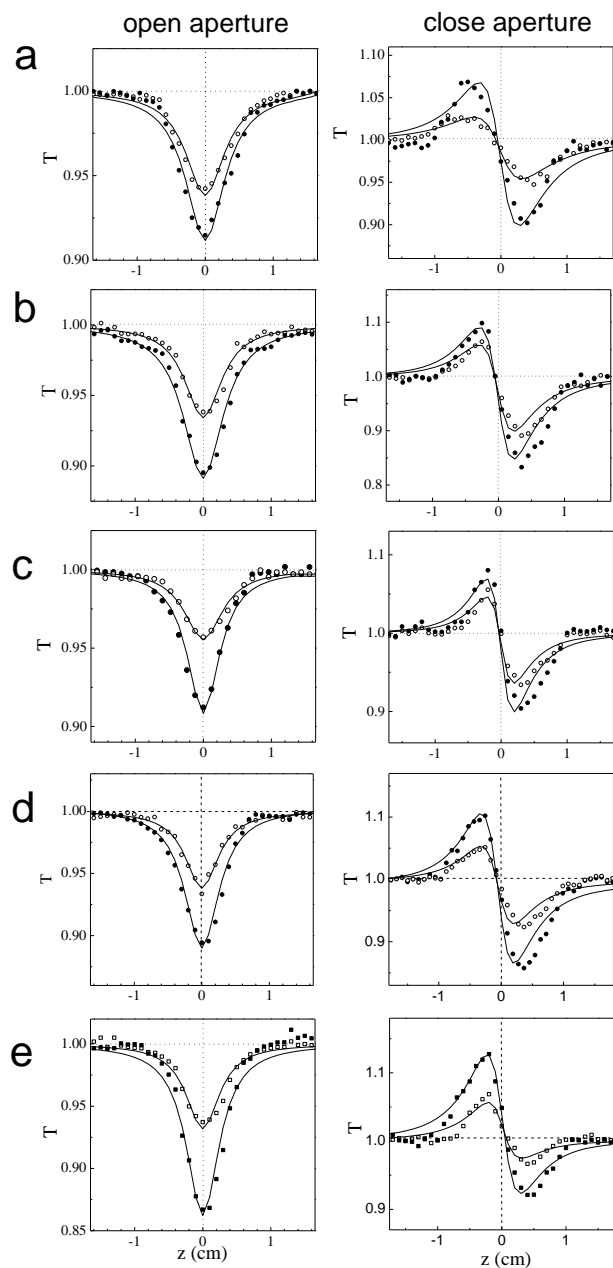


Figure SI-6. Z-scan data (symbols) and theoretically fitted curves (solid curves) of $[(\text{PbS})_{\text{QD}}, 2 \text{ C}^+]_{\text{Y}}$ for $\text{C}^+ = \text{H}^+$ (a), Li^+ (b), Na^+ (c), K^+ (d) and Rb^+ (e) obtained under the open and closed aperture conditions at 532 nm. Input irradiances at the focal point were 0.1 and 0.19 GW/cm^2 (a) (b) (c) and 0.05 and 0.1 GW/cm^2 (d) (e)

SI-7. Z-scan Data at 1064 nm

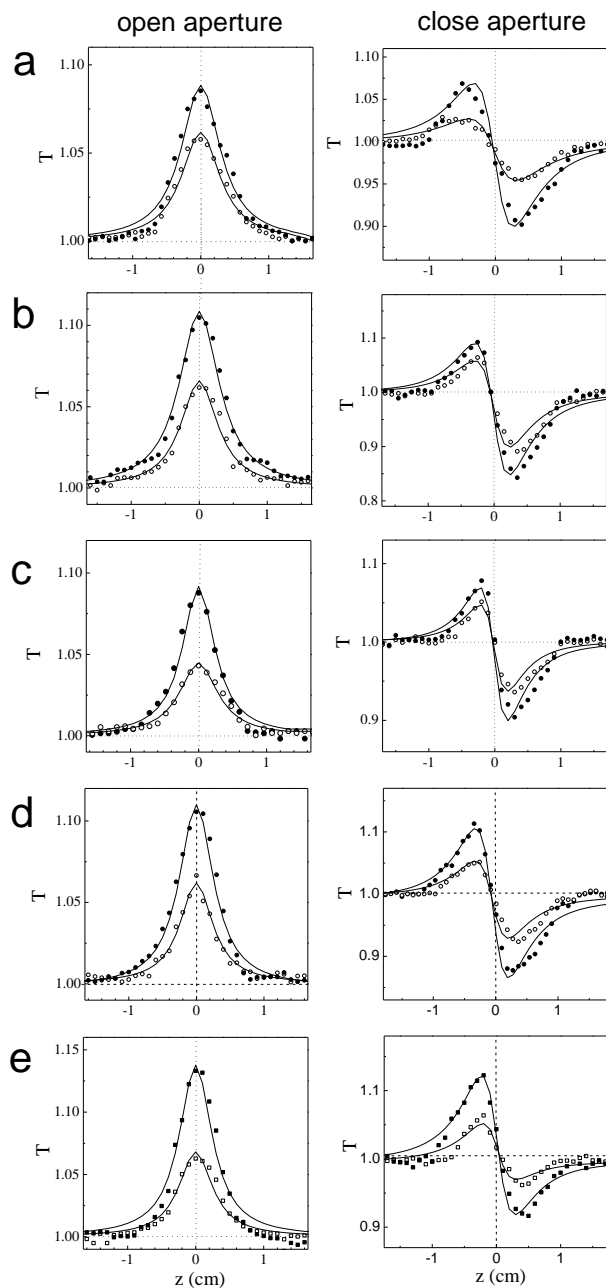


Figure SI-7. Z-scan data (symbols) and theoretically fitted curves (solid curves) of $[(\text{PbS})_{\text{QD}}, 2 \text{ C}^+]_{\text{Y}}$ for $\text{C}^+ = \text{H}^+$ (a), Li^+ (b), Na^+ (c), K^+ (d) and Rb^+ (e) obtained under the open and closed aperture conditions at 532 nm. Input irradiances at the focal point were 0.25 and 0.45 GW/cm^2 (a) (b) (c) and 0.14 and 0.23 GW/cm^2 (d) (e)

SI-8. Sanderson's Partial Negative Charge of Oxygen in the Zeolite Framework

Sanderson's intermediate electronegativity, S_z , of each M^+ -exchanged zeolite was calculated according to the equation,

$$S_z = (S_M^p S_{Si}^q S_{Al}^r S_O^t S_{Pb}^u S_S^v)^{1/(p+q+r+t+u+v)}$$

where, S_M , S_{Si} , S_{Al} , S_O , S_{Pb} , and S_S represent Sanderson's electronegativity values of the alkali metal cation, silicon, aluminum, oxygen, lead, and sulfur, respectively, and p , q , r , t , u , and v represent the number of the corresponding element, respectively, in a unit cell. The corresponding Sanderson's (average) partial charge of the framework oxygen, δ_o , was subsequently obtained using the following equation,

$$\delta_o = (S_z - S_O)/(2.08S_O^{1/2}).$$

Sanderson's electronegativity values used in this work are: Si = 2.14; Al = 1.71; O = 3.65; H = 2.59, Li = 0.89; Na = 0.56; K = 0.45; Rb = 0.31; Pb = 1.92; S = 2.96. The values were taken from Huheey, J. E.; Keiter, E. A.; Keiter, R. L. *Inorganic Chemistry*, 4th ed.; Harper Collins College Publications: New York, 1993; p 187 ff.

SI-9. Methods Used to Prepare Figure 4.

The illustrations were prepared by adopting zeolite X with the unit cell composition of $Si_{96}Al_{96}O_{384}M_{96}$ ($M = H, Li, Na, K, \text{ and } Rb$) as the model structure using universal force field and a materials studio modeling 5.5 package. Here, only the positions of the cations were optimized. An orange colored ball inside each supercage was added into the illustration to emphasize the space surrounded by the cations and framework.